

## OPTICAL PROPERTIES OF Bi DOPED Se-Te THIN FILMS

ANUP KUMAR<sup>a,c</sup>, PAWAN HEERA<sup>a</sup>, P. B. BARMAN<sup>b</sup>, RAMAN SHARMA<sup>a\*</sup>

<sup>a</sup>*Department of Physics, Himachal Pradesh University, Shimla-171005, India*

<sup>b</sup>*Department of Physics, Jaypee University of Information Technology, Waknaghat, Solan-173234, India*

<sup>c</sup>*Physics Department, Govt. Degree College, Kullu, H. P. 175101, India*

Compositional dependence of optical constants of thermally evaporated amorphous  $\text{Se}_{82-x}\text{Bi}_x\text{Te}_{18}$  ( $x = 0, 1.5, 2.5, 3.5$  and  $4.5$  at %) thin films has been studied using well established Swanepoel method. The optical parameters like, refractive index ( $n$ ), extinction coefficient ( $k$ ), film thickness ( $d$ ), absorption coefficient ( $\alpha$ ) and optical band gap ( $E_g$ ) etc. are determined from the transmission spectra in the spectral range from 500 to 2500 nm. Wemple-DiDomenico (WDD) single oscillator approach is used to study the dispersion parameters such as single-oscillator energy ( $E_0$ ), dispersive energy ( $E_d$ ) and static refractive index ( $n_0$ ). Present results show that the refractive index increases with the increasing concentration of Bi which is in agreement with the earlier studies. The increase in refractive index with Bi content may be ascribed to the increase in mean polarizability per atom of the system. The optical energy gap has been estimated by using Tauc's extrapolation method and is found to decrease with an increase in Bi concentration. The decrease in optical band gap can be understood in terms of decrease in cohesive energy and increase in electronegativity of the films under study.

(Received September 27, 2012; Accepted October 19, 2012)

*Keywords:* Optical properties, Chalcogenide glasses, Thin films, Refractive index, Optical conductivity.

### 1. Introduction

Chalcogenide glasses have drawn a great attention due to their unique properties and potential applications in modern technology [1]. These glasses are very promising materials for optical fibers, switching devices, gratings, optical amplifiers, optical memories, ultrafast optical switches, etc.[2-5]. Chalcogenide glasses are characterized by a relatively high atomic mass and a weak bond strength which results in low phonon energies. High transparency of these glasses in mid to far-IR region makes them very useful for their application in IR-window and optics [6]. The energy band gap of these glasses is considerably important and plays a major role in fabrication of the device for a particular wavelength. The energy gap in these materials can be modified to a considerable range by the addition of chemical impurities [7]. The optical properties of these glasses depend on their atomic and electronic band structure [8]. Addition of metal impurities has a considerable influence on the optical properties of chalcogenide materials. Among these glasses, selenide based glasses are of great interest due to their good glass-forming ability, property of reversible transformation and non-linear optical applications [9, 10]. Pure Se is a good glass former but is not stable in standard operational conditions. Binary Se-Te glasses have acquired the advantages of higher photosensitivity, greater hardens and moderate crystallization temperature [11-13]. To enhance thermal stability and glass-forming ability (GFA) of these materials different metallic impurities like In, Sb, Pb, Ge, Ag, Bi etc., are used as glass modifiers [14-16]. It is found that the addition of Bi changes the conductivity of the material from p- to n-type, expands the glass

---

\* Corresponding author: sramanb70@mailcity.com,

forming region and creates the configurational and compositional disorders in the alloys [17-19]. In the present work, our aim is to study the effect of Bi doping on the optical properties of  $\text{Se}_{82-x}\text{Bi}_x\text{Te}_{18}$  ( $x=0, 1.5, 2.5, 3.5$  and  $4.5$  at %) thin films. The optical parameters like, refractive index ( $n$ ), absorption coefficient ( $\alpha$ ), film thickness ( $d$ ), optical band gap ( $E_g$ ), etc. are determined from the transmission spectra in the spectral range of 500-2500 nm. The well known Swanepoel's method [20] based on Manifacier's idea [21] is used to estimate the optical constant from the transmission spectra. The dispersion parameters such as single-oscillator energy ( $E_0$ ), dispersive energy ( $E_d$ ) and static refractive index ( $n_0$ ) are studied in terms of Wemple-DiDomenico (WDD) single oscillator approach [22]. The optical energy gap has been estimated by using Tauc's extrapolation method [23] and is found to decrease with an increase in Bi content.

## 2. Experimental Details

The glassy alloys of  $\text{Se}_{82-x}\text{Bi}_x\text{Te}_{18}$  (for  $x= 0, 1.5, 2.5, 3.5$  and  $4.5$  at %) in bulk form were prepared by melt quenching technique. High purity (99.999%) elemental substances were weighed according to their atomic percentages and were sealed in quartz ampoule evacuated to a vacuum of  $10^{-5}$  torr. The sealed ampoules were heated in a vertical furnace at an appropriate temperature of  $900$  °C for 15 hours by gradually increasing the temperature at the rate of  $3-4$  °C per minute. The ampoules were rocked frequently, during heating, in order to ensure the homogenization of the melt. The ampoules were quenched in ice cooled water to obtain the glassy alloy. The samples were separated from the ampoules by dissolving the ampoules in  $\text{HF} + \text{H}_2\text{O}_2$  solution for about 48 h. Thin films were prepared on a well cleaned microscopic glass substrates by thermal evaporation technique [Vacuum coating unit HINDHIVAC 12A 4D Model], at a vacuum of  $10^{-5}$  torr. Separate molybdenum boat is used for each sample. The substrates were kept at room temperature. The films were grown at the rate of 13 Angstrom per second so as to achieve a film composition very near to the bulk material. The deposition parameters for all the films were kept same so that the results could be compared. The thin films were kept inside the deposition chamber for about 24 h to achieve a metastable equilibrium. The amorphous state of the thin films was again confirmed from the X-ray diffraction pattern. The transmission spectra of as-deposited films were measured by using ultraviolet-visible-near infrared double beam spectrophotometer [Perkin Elmer Lamda-750]. All the measurements were carried out at room temperature (300 K).

## 3. Results and Discussion

The XRD pattern of  $\text{Se}_{82-x}\text{Bi}_x\text{Te}_{18}$  ( $x=0, 1.5, 2.5, 3.5$  and  $4.5$ ) thin films is shown in Fig.1. The absence of sharp structural peaks in the XRD traces confirms the amorphous state of the films under study.

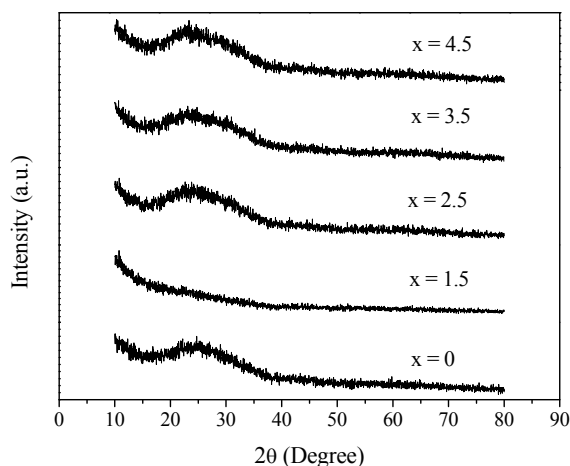


Fig. 1 XRD pattern of  $\text{Se}_{82-x}\text{Bi}_x\text{Te}_{18}$  ( $x= 0, 1.5, 2.5, 3.5$  and  $4.5$ ) thin films.

The transmittance  $T$  as a function of wavelength for  $\text{Se}_{82-x}\text{Bi}_x\text{Te}_{18}$  amorphous thin films is shown in Fig. 2. The occurrence of maxima and minima in the transmission spectra ensure the optical homogeneity of the films. The transmittance spectra, in Fig. 2, are found to shift towards higher wavelength with increasing concentration of Bi. This shift may be due to the addition of heavier Bi atoms to Se-Te matrix. Our results for the transmission spectra are similar to the results reported earlier [24, 25]. According to Swanepoel [20] an envelope is drawn through the extremes of each transmission spectrum using the origin version 6.0. Transmittance envelope functions  $T_M$  and  $T_m$ , i.e., transmission maxima and corresponding minima at a certain wavelength  $\lambda$  are determined from the envelope and are reported in table 1. The maximum absolute accuracy of  $T_M$  and  $T_m$  is about  $\pm 0.001$ .

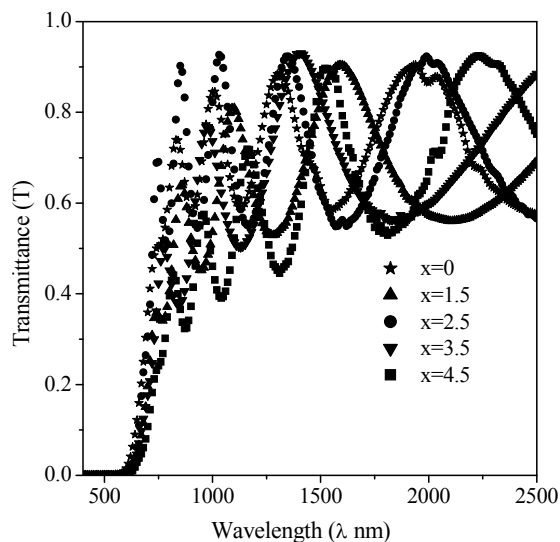


Fig. 2 Transmission spectra for  $\text{Se}_{82-x}\text{Bi}_x\text{Te}_{18}$  ( $x = 0, 1.5, 2.5, 3.5$  and  $4.5$ ) thin films.

### 3.1 Refractive index, film thickness and extinction coefficient

The optical constants like refractive index, film thickness and extinction coefficient, of  $\text{Se}_{82-x}\text{Bi}_x\text{Te}_{18}$  thin films are calculated from transmission spectra using the technique proposed by Swanepoel [20]. According to Swanepoel the refractive index  $n$  in the weak absorption region can be obtained from the relation

$$n = \left[ N + (N^2 - s^2)^{\frac{1}{2}} \right]^{\frac{1}{2}}, \quad (1)$$

Where

$$N = 2s \frac{T_M - T_m}{T_M T_m} + \frac{s^2 + 1}{2}. \quad (2)$$

In equation (1)  $s=1.5$  is the refractive index of the substrate. The calculated values of refractive index  $n_1$  for  $\text{Se}_{82-x}\text{Bi}_x\text{Te}_{18}$  thin films are given in table 1. From table 1 it is observed that the refractive index  $n_1$  decreases with an increase in the wavelength and increases with increasing concentration of Bi. The decrease in refractive index with wavelength shows the normal dispersion behavior of the material. The increase in refractive index with increasing concentration of Bi may be correlated with the increased density ( $\rho$ ) of the system [26, 27]. The addition of Bi ( $\rho = 9.80$



Bi at %	$\lambda$ (nm)	$T_M$	$T_m$	$n_1$	$d_1$ (nm)	$m_0$	$m$	$d_2$ (nm)	$n_2$
	1155	0.919	0.549	2.70	760.32	3.725	3.5	745.86	2.68
	1349	0.92	0.554	2.69	781.55	3.168	3	751.60	2.69
	1574	0.921	0.556	2.68	764.32	2.709	2.5	732.48	2.61
	1992	0.922	0.56	2.67		2.130	2	745.40	2.60
					$\bar{d}_1=793.92$			$\bar{d}_2=752.09$	
x=3.5	808	0.439	0.282	3.26		5.866	6	742.85	2.91
	873	0.498	0.318	3.13	665.60	5.220	5.5	765.28	2.89
	949	0.578	0.351	3.11	755.82	4.775	5	760.50	2.85
	1046	0.65	0.384	3.06	723.20	4.259	4.5	767.42	2.83
	1145	0.719	0.423	2.97	789.24	3.771	4	770.43	2.75
	1304	0.813	0.449	2.99	684.57	3.338	3.5	761.40	2.74
	1533	0.886	0.501	2.85	658.30	2.710	3	804.05	2.76
	1811	0.918	0.529	2.78	807.85	2.235	2.5	812.29	2.72
	2227	0.919	0.532	2.77		1.811	2	802.16	2.68
					$\bar{d}_1=726.37$			$\bar{d}_2=776.27$	
x=4.5	778	0.504	0.31	3.23		3.776	4	480.52	3.13
	865	0.653	0.372	3.15	482.60	3.310	3.5	479.53	3.05
	972	0.77	0.428	3.03	430.24	2.836	3	479.83	2.93
	1140	0.845	0.493	2.83	419.90	2.256	2.5	502.56	2.87
	1397	0.92	0.551	2.70	481.74	1.755	2	516.70	2.81
	1830	0.921	0.565	2.65		1.314	1.5	517.46	2.76
					$\bar{d}_1=453.62$			$\bar{d}_2=496.10$	

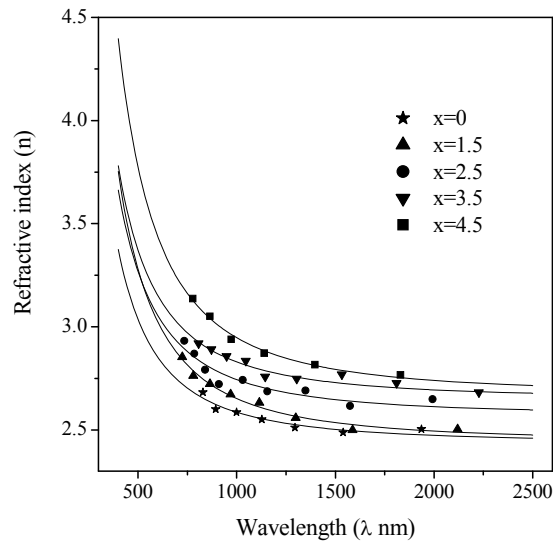


Fig. 3 Variation of refractive index ( $n$ ) with wavelength ( $\lambda$ ) for  $Se_{82-x}Bi_xTe_{18}$  ( $x=0, 1.5, 2.5, 3.5$  and  $4.5$ ) thin films.

If  $n_1$  and  $n_2$  are the refractive indices of two adjacent maxima (or minima) at wavelengths  $\lambda_1$  and  $\lambda_2$ , respectively, then the thickness of the film can be determined [20] from the relation

$$d = T_M \frac{\lambda_1 \lambda_2}{2(\lambda_1 n_2 - \lambda_2 n_1)}. \quad (5)$$

Here, for two adjacent maxima  $T_M = 1$ . The film thickness  $d_1$  is calculated from equation (5)

and the obtained values of film thickness are given in table 1. The average value of film thickness  $\overline{d}_1$  along with  $n_1$  and  $\lambda$  is used to determine the order number  $m_0$ , from equation (4), at different extremes of the transmission spectra. By taking the exact integer or half integer value of  $m$  the accuracy of film thickness can be increased significantly. The new film thickness  $d_2$  is obtained from equation (4) by using the values of  $n_1$  and  $m$  (integer and half integer for maxima and minima) for each value of  $\lambda$ . Values of new film thickness  $d_2$ ,  $m$  and  $m_0$  for the investigated thin film are also reported in tables 1. Now, using the exact value of  $m$  and film thickness  $\overline{d}_2$ , equation (4) can be solved for refractive index  $n$  at each  $\lambda$ . The new values of the refractive index  $n_2$  are fitted to the Cauchy's relation [30] i.e.,  $n_2 = a + b/\lambda^2$ , to extrapolate the values of the refractive index for all wavelengths as shown in Fig. 3.

The extinction coefficient  $k$ , appearing in the complex refractive index i.e.,  $n^* = n + ik$ , is the measure of the fraction of light lost due to scattering and absorption per unit distance of the medium. It can be expressed [20] in terms of absorption coefficient  $\alpha$  through the equation

$$k = \frac{\lambda}{4\pi d} \ln\left(\frac{1}{x}\right), \quad (6)$$

where  $d$  is the film thickness and  $x$  is the absorbance. The absorbance in the weak and medium absorption region can be calculated from the relation

$$x = \frac{E_M - \left[ E_M^2 - (n^2 - 1)^3 (n^2 - s^4) \right]^{\frac{1}{2}}}{(n - 1)^3 (n - s^2)}, \quad (7)$$

with

$$E_M = \frac{8n^2s}{T_M} - (n^2 - 1)(n^2 - s^2) \quad (8)$$

The extinction coefficient  $k$  for the investigated thin films is calculated from equation (6). The extinction coefficient as a function of wavelength is plotted in Fig. 4.

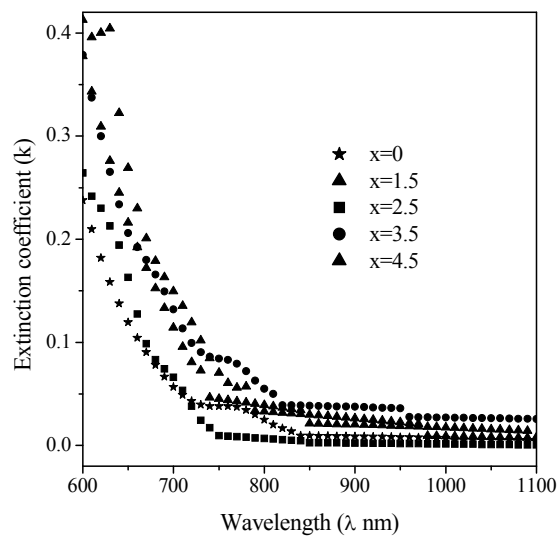


Fig. 4 Variation of extinction coefficient ( $k$ ) with wavelength ( $\lambda$ ) for  $Se_{82-x}Bi_xTe_{18}$  ( $x = 0, 1.5, 2.5, 3.5$  and  $4.5$ ) thin films.

Fig. 4 shows that the extinction coefficient decreases with increase in wavelength which implies that the fraction of light lost due to scattering decreases with an increase in the wavelength. Our results for  $k$  are in agreement with the earlier reported results for Bi doped thin films [25].

### 3. 2 Dispersion energy, oscillator strength and static refractive index

The energy dispersion of refractive index  $n$  has been studied by using Wemple-DiDomenico model [31]. According to WDD model the refractive index can be described to an excellent approximation by the relation

$$n^2 - 1 = \frac{E_d E_0}{E_0^2 - E^2}, \quad (9)$$

where  $E = h\nu$  is the photon energy,  $E_0$  is the energy of the effective dispersion oscillator (average energy gap) and  $E_d$  is the dispersion energy which is a measure of the interband optical transitions. The oscillator parameters  $E_0$  and  $E_d$  are calculated by plotting  $(n^2-1)^{-1}$  versus  $E^2$  and fitting the data in a straight line to the points as shown in Fig. 5. The values of the dispersion parameters  $E_0$  and  $E_d$  are determined from the slope  $1/(E_0 E_d)$  and the intercept  $E_0/E_d$  on the vertical axis. The calculated values of  $E_0$  and  $E_d$  are given in table 2. The dispersion parameter  $E_0$  decreases with an increase in Bi content whereas  $E_d$  is increases.  $E_0$  is related to the optical band gap  $E_g$  (calculated in the section 3.3) through an empirical relation proposed by Tanaka [32]. i.e.,

$$E_0 \approx 2E_g. \quad (10)$$

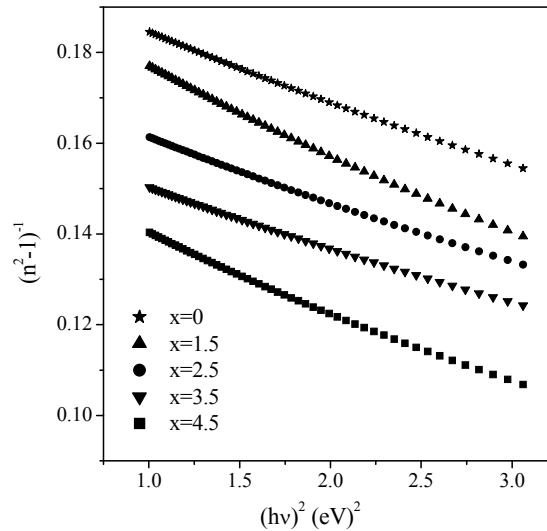


Fig. 5 Variation of refractive index factor  $(n^2-1)^{-1}$  versus  $(h\nu)^2$  for  $Se_{82-x}Bi_xTe_{18}$  ( $x = 0, 1.5, 2.5, 3.5$  and  $4.5$ ) thin films.

From table 2, it is deduced that the Tanaka's relation is valid for the investigated thin films as in case other chalcogenide glasses [25, 33]. Static refractive index ( $n_0$ ) and high frequency dielectric constant ( $\epsilon_\infty$ ) can be obtained from equation (10) by using the values of  $E_0$  and  $E_d$ . In the limit  $h\nu$  approaches to zero, equation (9) reduces to

$$n_0 = \left( 1 + \frac{E_d}{E_0} \right)^{\frac{1}{2}}. \quad (11)$$

The calculated values of static refractive index ( $n_0$ ) and high frequency dielectric constant ( $\epsilon_\infty = n_0^2$ ) are reported in table 2 and are found to increase with an increase in Bi content.

Table 2: Values of absorption coefficient ( $\alpha$ ) at 700 nm, dispersion energy ( $E_d$ ), oscillator energy ( $E_0$ ), static refractive index ( $n_0$ ), high frequency dielectric constant ( $E_\infty$ ) and optical band gap ( $E_g$ ) in  $Se_{82-x}Bi_xTe_{18}$  ( $x = 0, 1.5, 2.5, 3.5$  and  $4.5$ ) thin films.

Bi (at%)	$\alpha \times 10^4$ (cm <sup>-1</sup> )	$E_d$ (eV)	$E_0$ (eV)	$n_0$	$E_\infty$	$E_g$ (eV)
0	1.03	17.85	3.54	2.46	6.05	1.686
1.5	2.09	18.09	3.34	2.53	6.40	1.656
2.5	2.17	20.16	3.32	2.65	7.02	1.617
3.5	2.26	21.75	3.10	2.83	8.01	1.583
4.5	2.54	22.46	3.06	2.89	8.35	1.547

### 3.3 Absorption Coefficient and optical band gap

The absorption coefficient  $\alpha$  for  $Se_{82-x}Bi_xTe_{18}$  thin films can be calculated from the transmission spectra using the relation [20],

$$\alpha = \frac{1}{d} \exp\left(\frac{1}{x}\right), \quad (12)$$

here  $x$  is the absorbance of the material [20]. The value of absorption coefficient  $\alpha$  at a wavelength of 700 nm is given in table 2. From table 2 it is evident that the absorption coefficient increases with an increase in Bi concentration. The increase in the value of absorption coefficient with energy implies that the charge carriers have absorbed more energy and thus give rise to high value of absorption coefficient.

The absorption edge in amorphous semiconductors have three distinct regions, namely, high absorption region ( $\alpha = 10^4$  cm<sup>-1</sup>), an exponential edge region ( $\alpha = 10^2$ - $10^4$  cm<sup>-1</sup>) and a weak absorption tail region ( $\alpha \leq 10^2$  cm<sup>-1</sup>). The high absorption region is caused by the band to band transition and determines the optical band gap. The optical band gap ( $E_g$ ) in amorphous materials can be determined by using a well known relation [20] proposed by Tauc, i.e.,

$$\alpha h \nu = B (h \nu - E_g)^p, \quad (13)$$

here  $B$  is the slope of the Tauc edge called band tailing parameter. The value of the band tailing parameter  $B$  depends upon the width of the localized states in the band gap that are attributed to the homopolar bonds present in the chalcogenide glasses and is expressed as

$$B = \frac{(4\pi/c)\sigma_o}{n_o \Delta E}, \quad (14)$$



here  $n_0$  is the static refractive index,  $\Delta E$  is the located-state tail width,  $c$  is the velocity of light in vacuum and  $\sigma_0$  is the minimum metallic conductivity. The exponent  $p$  in equation (13) determines the type of transition.  $p=1/2, 2, 3/2$  and  $3$  correspond to the direct allowed transition, indirect allowed transitions, forbidden transition and indirect forbidden transitions, respectively. It is found that  $p=2$  provide a best fit for the optical absorption data in many chalcogenide glassy materials [34].  $(\alpha h\nu)^{1/2}$  as a function of photon energy  $E_e = h\nu$  for  $\text{Se}_{82-x}\text{Bi}_x\text{Te}_{18}$  thin films is shown in Fig. 6. The non-linear shape of the plots shows the indirect type of transition in the forbidden gap.

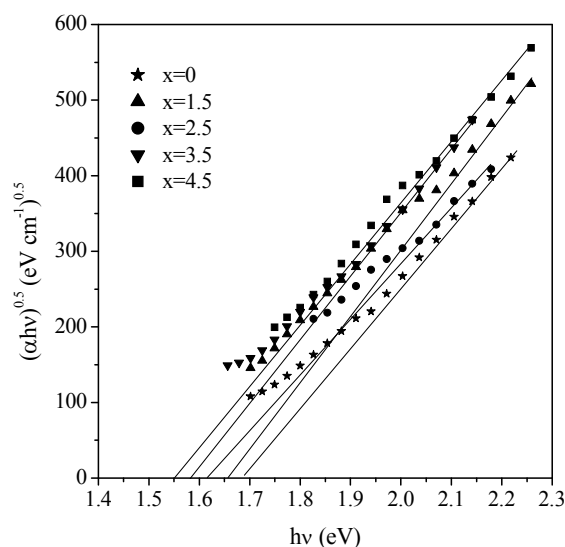


Fig.6 Variation in  $(\alpha h\nu)^{0.5}$  with photon energy ( $h\nu$ ) for  $\text{Se}_{82-x}\text{Bi}_x\text{Te}_{18}$  ( $x=0, 1.5, 2.5, 3.5$  and  $4.5$ ) thin films.

The optical energy gap for the indirect allowed transition is evaluated from the intercept by making  $(\alpha h\nu)^{1/2} \rightarrow 0$ . The obtained values of the energy band gap are given in table 2. From table 2 it is observed that the optical band gap decreases from 1.686 to 1.547 eV with an increase in Bi concentration. The similar trends in optical band gap have been observed earlier [25, 35]. Table 2 shows that the values of optical band gap obtained from the Tauc's relation are in good agreement with the values obtained from Tanaka's relation. The decrease in optical band gap may be explained in terms of the electronegativity difference of the elements involved. The valence band in chalcogenide glasses is constituted by lone pair p-orbital's [36] contributed by the chalcogen atoms. The lone pair electrons adjacent to electropositive atoms will have higher value of energies than those adjacent to electronegative atoms. The addition of electropositive atom raises the energy of lone pair states which broadens the valence band inside the forbidden gap. As the electronegativity values of Bi (2.02) is less than Se (2.55), so the addition of Bi may raise the energy of some lone pair states and broaden the valence band and hence, results in the reduction of optical band gap. Further, the decrease in optical band gap can also be correlated to the decrease in cohesive energy (CE) [37]. The decrease in the CE energy tends to decrease the energy of conduction band edge, which causes a reduction in the gap between bonding and anti-bonding orbitals and thus results in the decrease in the optical band gap. Lesser the cohesive energy means lower the bonding strength and hence reduction in the optical band gap. The decrease in the optical band gap may also be explained on the basis of the model for the density of states in an amorphous solid, proposed by Mott and Davis [38]. According to this model, the width of the localized states near the mobility edges depends on the degrees of disorder and defect states presented in the amorphous material. The addition of Bi in the Se-Te matrix introduces the large number of defects in the system. The presence of a high concentration of localized states in the band structure is responsible for the essential narrowing of optical band gap.

### 3.4 Dielectric constant and optical conductivity

The dielectric constant is a fundamental property of the material and it affects the movement of the electromagnetic signals through the materials. The material with high dielectric constant will make the light to travel slowly. The dielectric constant is a complex quantity and the real part of the dielectric constant explains that by how much amount the material will slow down the speed of light when passed through it and the imaginary part of the dielectric constant shows that how a dielectric material absorbs the energy from electric field due to dipole orientation. The values of refractive index and extinction coefficient obtained above are used to determine [39] the dielectric response of the material. The real part of the dielectric constant ( $\epsilon'$ ) is calculated by using the relation

$$\epsilon' = n^2 - k^2, \quad (15)$$

while imaginary part of the dielectric constant ( $\epsilon''$ ) is determined from the relation,

$$\epsilon'' = 2nk. \quad (16)$$

The values of the real and imaginary part of the dielectric constants for  $\text{Se}_{82-x}\text{Bi}_x\text{Te}_{18}$  thin films are given in table 3. From table it is evident that the real and imaginary part of the dielectric constant increases with increasing content of Bi. The knowledge of real and imaginary part of the dielectric constant gives the dissipation factor  $\tan(\delta)$  and is defined as  $\tan(\delta) = \epsilon''/\epsilon'$ . The calculated values of dissipation factor are also reported in table 3.

Optical conductivity ( $\sigma$ ) of the thin films directly depends on the refractive index and absorption coefficient of the material. It shows the optical response of the material and has the dimension of the frequency which are valid only in Gaussian system of units. The optical conductivity for thin films is calculated by using the relation [40].

$$\sigma = \frac{\alpha nc}{4\pi}, \quad (17)$$

where  $c$  is the velocity of light. The values of optical conductivity for thin films at a wavelength 700 nm are listed in Table 3. The plot of optical conductivity ( $\sigma$ ) as a function of photon energy ( $h\nu$ ) is shown in Fig. 7.

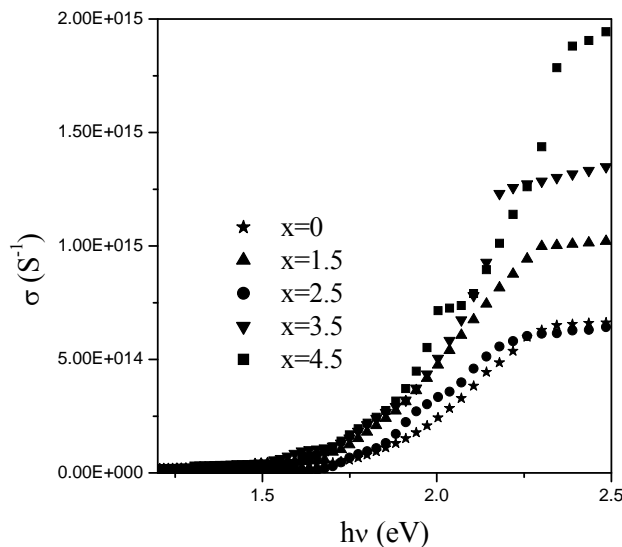


Fig.7 Variation of optical conductivity ( $\sigma$ ) with photon energy ( $h\nu$ ) for  $\text{Se}_{82-x}\text{Bi}_x\text{Te}_{18}$  ( $x=0, 1.5, 2.5, 3.5$  and  $4.5$ ) thin films.

Table 3: Values of dielectric constants ( $\epsilon'$  and  $\epsilon''$ ), optical conductivity ( $\sigma$ ) and dissipation factor  $Tan(\delta)$  for  $Se_{82-x}Bi_xTe_{18}$ , ( $x = 0, 1.5, 2.5, 3.5$  and  $4.5$ ) thin films.

Bi (at%)	$\epsilon'$	$\epsilon''$	$\sigma$ ( $s^{-1}$ )	$Tan(\delta)$
0	7.172	0.307	$6.596 \times 10^{13}$	0.0429
1.5	7.480	0.638	$1.368 \times 10^{14}$	0.0853
2.5	8.529	0.754	$1.304 \times 10^{14}$	0.0860
3.5	11.368	0.853	$1.827 \times 10^{14}$	0.0868
4.5	12.953	1.021	$2.188 \times 10^{14}$	0.0878

From Fig. 8 it is found that the optical conductivity increases with an increase in energy as well as Bi content. Since  $\sigma$  is directly related to the absorption coefficient and refractive index. Hence, increase in optical conductivity may be ascribed to the large absorption coefficient and refractive index. The increase in the value of optical conductivity may also be due to the increased density of localized states in the gap [41].

#### 4. Conclusions

The optical parameters of ternary  $Se_{82-x}Bi_xTe_{18}$  thin films for different compositions have been studied using normal incidence transmission spectra in the spectral range 500 nm-2500 nm. The optical parameters are determined by using Swanepoel's envelope method based upon Manifacier idea. Present results show that the refractive index ( $n$ ) increases, over the entire spectral range, with increasing concentration of Bi. The increase in the refractive index may be interpreted in terms of the increased polarizability of larger Bi atomic radius as compared to the other constituent elements in the composition. The Wemple-DiDomenico model has been used to determine dispersion parameters  $E_0$ ,  $E_d$  and  $n_0$ . It is found that the single oscillator energy  $E_0$  decreases with an increase in Bi concentration whereas dispersion energy  $E_d$  and static refractive index  $n_0$  are found to increase with increasing Bi content. The oscillator energy  $E_0$  is found to satisfy the Tanaka's empirical relation for the optical band gap  $E_g$ . The optical band gap  $E_g$  has been estimated by using Tauc's nondirect transition model and is found to decrease with an increase in Bi content in ternary thin films. The decrease in the optical band gap is correlated with decrease in the cohesive energy of the system. The real and imaginary part of the dielectric constant ( $\epsilon$ ) and optical conductivity  $\sigma$  are also found to increase with the increasing concentration of Bi in the films under consideration.

#### References

- [1] R. Naik, A. Jain, R. Ganesan and K. S. sangunni, Thin Solid Films **520**, 2510 (2012).
- [2] M. Ahmad, R. Thangaraj and T. S. Sathiaraj, J. Mater. Sci. **45**, 1231 (2010).
- [3] G. Wang, Q. Nie, M. Barj, X. Wang, S. Dai, X. Shen, T. Xu and X. Zhang, J. Phys. And Chem. Of Solids **72**, 5 (2011).
- [4] A. A. Bahishti, M. A. Majeed Khan and B. S. Patel, J. Non-Cryst. Solids **355**, 2314 (2009).
- [5] V. Pamukchieva, A. Szekeres and K. Todorova, J. Non-Cryst. Solids **355**, 2485 (2009).
- [6] P. Sharma and S. C. Katyal, Thin Solid Films **517**, 3813 (2009).
- [7] E. Marquez, T. wagner, J. M. Gonzalez-Leal, A. M. Bernal-Olive, R. Prieto-Aleon, R. Jimenez-Garay, P. J. S. Ewen, J. Non-Cryst. Solids **274**, 62 (2000).
- [8] E. R. Shaaban, Phil. Mag. **88**, 781 (2008).
- [9] H. Nasu, R. Kubodera, M. nakamura and K. Kamiya, J. Am. Ceram. Soc. **73**, 1794 (1990).
- [10] G. Singh, J. Sharma, A. Thakur, N. Goyal, G. S. S. Saini and S. K. Tripathi, J. Optoelectron. Adv. Mater. **7**, 2069 (2005).
- [11] Z. Wang, C. Tu, Y. Li, Q. Chen, J. Non-Cryst. Solids **191**, 132 (1995).

- [12] H. Yang, W. Wang, S. Min, *J. Non-Cryst. Solids* **80**, 503 (1986).
- [13] A. S. Soltan, M. Abu EL-Oyoun, A.A. Abu-Sehly, A.Y. Abdel-Latif, *Mater. Chem. Phys.* **82**, 101 (2003).
- [14] A. Khan Shamshad, M. Zulfequar, M. Husain, *Curr. Appl. Phys.* **5**, 583 (2005).
- [15] L.A. Kulakova, V. Kh. Kudoyarova, B.T. Melekh, V.I. Bakharev, *J. Non-Cryst. Solids* **352**, 1555 (2006).
- [16] M. Hrdlicka, J. Prikryl, M. Pavlista, L. Benes, M. Vlcek, M. Frumar, *J. Phys. Chem. Solids* **68**, 846 (2007).
- [17] E. R. Shaaban, M.T. Dersouky and A. M. Abousehly, *Phil. Mag.* **88**, 1099 (2008).
- [18] P. Nagels, M. Rotti and W. Vukobratovic, *J. Phys. (Paris)* **42**, 907 (1981).
- [19] N. Tohge, T. Minami and M. Tanaka, *J. Non-Cryst. Solids* **59-60**, 1015 (1983).
- [20] R. Swanepoel, *J. Phys. E.Sci. Instrum.* **16**, 1214 (1983).
- [21] J. C. Manifacier, J. Gasiot and J. P. Fillard, *J. Phys. E. Sci. Instrum.* **9**, 1002 (1976).
- [22] S. H. Wemple and M. DiDomenico, *Phys. Rev. B* **3**, 1338 (1971).
- [23] J. Tauc, In *Amorphous and liquid semiconductors*, ed. By J. Tauc (Plenum Press, Newyork,(1979).
- [24] Mainika, P. Sharma, S. C. Katyal and N. Thakur, *J. Non-oxide Glasses* **1**, 90 (2009).
- [25] K. Kumar, P. Sharma, S. C. Katyal and N. Thakur, *J. Phys. Scr.* **84**, 045703 (2011).
- [26] K. Vedam and P. Limsuwan, *J. Chem. Phys.* **69**, 4772 (1978).
- [27] C. Z. Tan and J. Arndt, *Physica B* **229**, 217 (1997).
- [28] E. Marquez, J. M. Gonzalez-Leal, A. M. Bernal-Oliva, R. Jimenez-Garay, and T. Wagner, *J. Non-Cryst. Solids* **354**, 503 (2008).
- [29] S. R. Elliot, *The Physical and chemistry of Solids* (Wiley, Chichester, 2000).
- [30] T. S. Moss, *Optical Properties of Semiconductors*, (London: Butterworth), 1959.
- [31] S. H. Wemple and M. DiDomenico, *Phys. Rev. B* **3**, 1338 (1971).
- [32] K. Tanaka, *Thin Solid Films* **66**, 271 (1980).
- [33] P. Sharma, I. Sharma and S. C. Katyal, *J. Appl. Phys.* **105**, 053509 (2009).
- [34] N. F. Mott and E. A. Davis, *Electronic Processes in Non-Crystalline Materilas*, (Clarendon Press, Oxford, 1971).
- [35] A. Sharma and P. B. Barman, *J. Thin Solid Films* **517**, 3020 (2009).
- [36] M. Kastner, D. Alder and H. Fritzsche, *Phys. Rev. Lett.* **35**, 1504 (1976).
- [37] A. Kumar, P. B. Barman and Raman Sharma, *Adv. In Appl. Sci. Research* **1**(2), 47 (2010).
- [38] N. F. Mott and E. A. Davis, *Electronic Processes in Non-Crystalline Materials*, Clarendon Press, Oxford, 382/ 428 (1979).
- [39] A. Goswami, *Thin Film Fundamental*, New Age International, New Delhi, 2005.
- [40] J. I. Pankov, *Optical Processes in Semiconductors*, Dover, New York, 1975.
- [41] N. F. Mott and E. A. Davis *Phil. Mag.* **22**, 903 (1970).